heritage

MDPI

Article

Ultramarine Blue in Edvard Munch's Collection: A Multi-Analytical Study of Early 20th Century Commercial Oil Paints

Beatrice G. Boracchi [1], Eun-Jin Strand Ferrer [1], Margherita Gnemmi [2], Laura Falchi [2], Francesca Caterina Izzo [2] and Irina Crina Anca Sandu [1,*]

[1] MUNCH, Conservation Section, Edvard Munchs Plass, 1, 0194 Oslo, Norway; beatrice.boracchi@munchmuseet.no (B.G.B.); jin.ferrer@munchmuseet.no (E.-J.S.F.)
[2] Conservation and Heritage Science Group, Ca' Foscari University of Venice, Via Torino, 155/b, Mestre, 30173 Venice, Italy; margherita.gnemmi@unive.it (M.G.); laura.falchi@unive.it (L.F.); fra.izzo@unive.it (F.C.I.)
* Correspondence: irina.sandu@munchmuseet.no

Abstract: The recurrence of specific deteriorating phenomena in blue paints used by Edvard Munch, observed more frequently from artworks from 1907 and onwards, calls for an analytical investigation of these paints. Ten commercial Ultramarine blue oil paint tubes from Munch's studio materials were studied, employing a multi-analytical approach comprising ATR-FTIR, μ-Raman, GC-MS, and SEM-EDS techniques. This study aims to ascertain the composition of these industrially produced blue oil paints and shed more light on the potential implications for darkening and other deterioration phenomena observed in Munch's artworks. The analyzed samples exhibited complex mixtures, characterized by significant presences of additives such as non-drying or partially drying oils, metal soaps, and preservatives. Moreover, extenders including clay minerals and white and other blue pigments were identified. Some compositions diverged from those indicated on the labels of the tubes. This study presents hypotheses regarding the causes of deterioration mechanisms observed in Ultramarine blue paints and outlines future perspectives and implications of darkening and other surface degradation phenomena in paintings from MUNCH's collection towards best conservation and display practices.

Keywords: ultramarine blue; Edvard Munch; modern oil paints; investigation

Citation: Boracchi, B.G.; Ferrer, E.-J.S.; Gnemmi, M.; Falchi, L.; Izzo, F.C.; Sandu, I.C.A. Ultramarine Blue in Edvard Munch's Collection: A Multi-Analytical Study of Early 20th Century Commercial Oil Paints. *Heritage* **2024**, *7*, 4027–4044. https://doi.org/10.3390/heritage7080190

Academic Editors: Georgios P. Mastrotheodoros, Eleni Kouloumpi and Anastasia Rousaki

Received: 14 June 2024
Revised: 15 July 2024
Accepted: 18 July 2024
Published: 31 July 2024

1. Introduction

The present study arises from the observation of darkening and other degradation phenomena in some areas of Edvard Munch's paintings containing Ultramarine blue oil paints. Two paintings from the MUNCH museum's collection—*Old Man in Warnemünde* (1907) and *The Drowned Boy* (1907–1908)—were investigated using Hirox 3D microscopy (Figures 1 and 2). It has been observed that in areas in which Ultramarine blue paint had been applied directly from the tube to the canvas, a specific darkening had occurred. In both paintings, the extensive use of Ultramarine blue paints had been identified from previous investigations [1–3]. Additionally, problems of adhesion with the underlying layers were observed, resulting in extensive cracking and losses, as well as the aforementioned darkening of the superficial layer of these thick blue paint strokes, resulting in an almost black skin on top of the pristine color (Figure 2).

Previous studies focusing on these two paintings set the basis for looking into these phenomena [1,2], but the complete understanding of the mechanism regulating them is far from being achieved. The present article sheds light on the composition in terms of pigments, binding media, additives, and adulterants of ten Ultramarine blue oil paint tubes from MUNCH's collection. Although we are not sure that the analyzed paint tubes have been used specifically for these paintings, this approach can be useful to establish possible factors that affect the stability of the paint materials over time and will add information on the composition of early industrially manufactured oil paints.

Figure 1. (**Left**): *The Drowned Boy* (1907–1908), oil on canvas, 86 × 130.5 cm; (**right**): *Old Man in Warnemünde* (1907), oil on canvas, 110.5 × 81 cm. Photos: MUNCH, photo-archive.

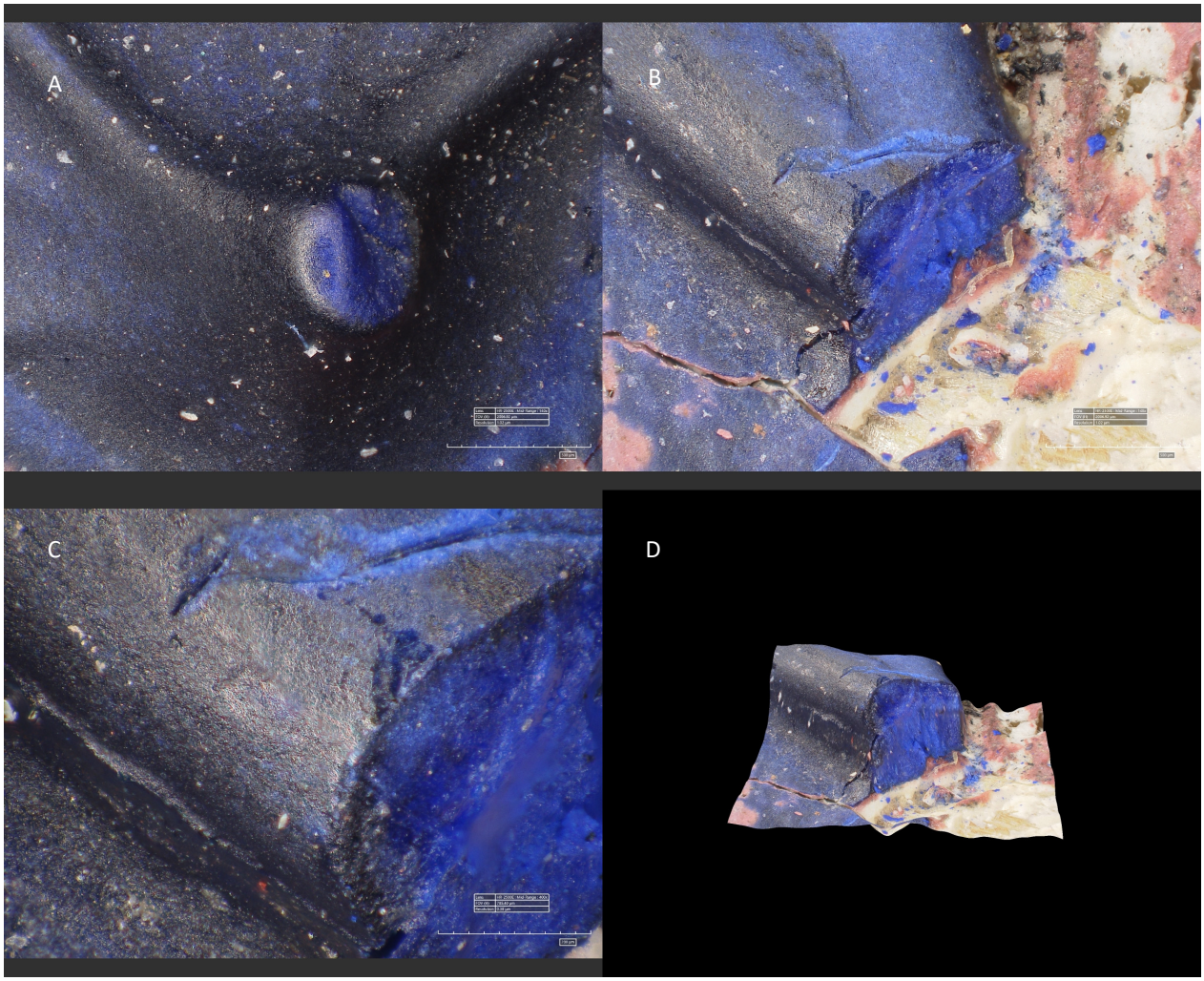

Figure 2. Details from *Old Man in Warnemünde*, showing dirt accumulation, darkening, cracking, and loss of cohesion. (**A**) Detail from the bottom part of the stylized blue figure in the background, 140×; (**B**,**C**) detail from the jacket of the stylized blue figure in the background, 140× and 400×; (**C**) 3D rendering of detail represented in image (**D**).

The paint tubes had been produced and sold by manufacturers from different countries, some from well-known and still existing paint manufacturers, like Winsor & Newton, while others were from now-obscure brands like Ambor (France, Paris), manufactured by Morin et Janet [4] (Figure 3).

Figure 3. Five of the paint tubes from MUNCH's collection, owned by the artist himself. The paint tubes were in different conservation states, from used and dried out to well preserved and almost untouched.

1.1. Industrial Manufacturing of Modern Paints

Following the invention of the collapsible metal tube in 1841 [5], commercial paint production began to flourish, and with it the secrets behind the formulation of these new materials, often protected by industry patents. In fact, the otherwise quite simple and well-known composition of the traditional mediums of oil mixtures of the previous times became increasingly complex, with the addition of additives (e.g., stabilizers, dispersion agents, fillers, extenders) and the synthesis of new colorants and pigments in order to extend the shelf life, maintain specific handling properties, accelerate the time of drying of the paint, and cut the costs of production [6]. Moreover, in addition to the customary siccative oils like linseed, poppyseed, and walnut oils, alternative drying or semi-drying binders were frequently utilized, often as economical alternatives to linseed oil [6]. These modifications to the paint composition significantly impacted the eventual properties and performance of oil films, occasionally resulting in adverse effects and unforeseen alterations to certain colors. Various authors have linked these outcomes to the interplay among the diverse components of the updated formulations [1,6–8].

1.2. An Overview on Ultramarine Blue Pigment

Ultramarine blue is a pigment that has been in the artists' palettes since ancient times [9]. In early times, the source used to obtain the pigment was lapis lazuli, a semi-precious stone imported from Afghanistan.

Due to its noble and remote origin, Ultramarine Blue has always been an extremely expensive and prestigious color, until a synthetic version was made available on the market in 1828 due to the discovery made by Jean Baptiste Guimet in France [9,10], and by Gmelin in Germany around the same time [8]. Starting from this date, the rise of this synthetic substitute marked a sharp decline in the use of the natural mineral-based pigment [9]. The synthetic pigment composition is namely the same as the one of lazurite mineral, $Na_{6–10}Al_6Si_60_{24}S_{2–4}$, but capable of considerable variation according to the ratio of the starting materials used in the manufacture and the conditions of preparation [9,10].

There are two main manufacturing methods for producing synthetic ultramarine: the first, named 'Soda Ultramarine', is made by heating a ground mixture of China clay, soda

ash, coal or charcoal, and sulfur for 12 to 18 h in closed crucibles (reducing atmosphere) [11]; the second, known as 'Sulfate Ultramarine', is produced by using sodium sulfate in place of soda ash [9,11]. This latter pigment has a greenish tinge. The purity of the ingredients is of great importance, especially regarding the absence of iron [9] and excess of readily reacting sulfur, which have been suggested to be connected to blackening of the pigment in early experiments [8].

Both artificial and natural Ultramarine blue exhibit a good lightfastness and share most of their chemical properties. They have quite good resistance to ammonia or caustic alkalis, but they are readily decomposed in the presence of acids, liberating sulfuric acid and leaving a yellowish glassy matrix of undissolved silica [9]. This phenomenon, caused by the entering of H_3O^+ ions into the open matrix of the mineral and the interaction with the enclosed polysulfide ions, seems to occur more readily in the synthetic pigment, but it has yet not been established if this occurs because of the coarser particle size of the natural pigment [9]. This effect might be the cause of the "Ultramarine sickness" observed by different authors [9,11–14], in which the bleaching of the blue color towards light gray tones might be due to the interactions between the paint and atmospheric sulfur and moisture.

Other studies attribute Ultramarine disease, described as the blanching or fading of Ultramarine blue areas, to the interaction between the oil paint medium and the pigment, either through the intrinsic acidity of the oil itself [9] or through the photocatalytic properties of Ultramarine pigment as a zeolite mineral to degrade the binding medium in the presence of UV radiation, leading to light scattering and the observed changes in reflectance [12]. Even if numerous studies concerning the stability and fading of Ultramarine blue have been carried out [11–14], fewer attempts have been made to explain the darkening reported in the literature and in the present study [1,2,15,16].

2. Experimental Section

The analytical methodology used complementary non-invasive and micro-invasive analytical techniques to gather relevant information from both the paintings and the paint tube samples.

2.1. Sampling

Ten samples were obtained from the selected Ultramarine blue tubes and analyzed with several techniques, as shown in Table 1.

Table 1. List of paint tubes and analyses.

Tube ID	Color on Label	Binder on Original Label	Brand	Production Coutry	Analyses Performed
MM.I.01638	Blau outremer extra	oil	Ambor	France	ATR-FTIR, μ-RAMAN, GC-MS
MM.I.1632	Blau outremer extra	oil	Ambor	France	ATR-FTIR, μ-RAMAN, GC-MS
MM.I.02126	Outremer N 2 clair	oil	Lefranc	France	ATR-FTIR, μ-RAMAN, GC-MS
MM.I.01959	Bleu d'outremer	oil	Blockx Fils	Belgium	ATR-FTIR, μ-RAMAN, GC-MS
MM.I.02219	Ultramarin dunkel	oil	Mussini Ölfarben Schmincke	Germany	ATR-FTIR, μ-RAMAN, GC-MS, SEM-EDS
MM.I.02330	Ultramarin, extra	oil	Vilhem Pacht	Denmark	ATR-FTIR, μ-RAMAN, GC-MS
MM.I.02384	Light ultramarin	oil	Winsor & Newton	England	ATR-FTIR, μ-RAMAN, GC-MS
MM.I.02387	Brilliant ultramarin	oil	Winsor & Newton	England	ATR-FTIR, μ-RAMAN, GC-MS
MM.I.02354	Brilliant ultramarin	oil	Winsor & Newton	England	ATR-FTIR, μ-RAMAN, GC-MS
MM.I.02424	Deep ultramarine	oil	Winsor & Newton	England	ATR-FTIR, μ-RAMAN, GC-MS

2.2. Hirox 3D Microscope Acquisition

Images of investigated areas in the selected case studies were acquired with a Hirox 3D Digital Microscope HRX-01, mounted on an ST-T500 Horizontal T-Stand 500 mm × 500 mm, allowing inspection and automated XYZ scanning of objects placed vertically. Two different sets of lenses were used: HR-1020E Telecentric polarized lenses for acquiring the scans ranging from 10× to 90× magnification, and HR-2500E ranging from 20× to 2500× magnification for acquiring smaller details. The HRX-01 software controls the motorized

XY and Z axis to achieve automated stitching (gigapixel panorama) as well as 3D depth maps using focus variation (also called focus stacking).

2.3. ATR-FTIR Spectroscopy

Spectra were acquired with an Alpha II Bruker spectrometer, in the spectral range from 4000 to 400 cm^{-1}, using a synthetic diamond crystal for the compression of the samples. The background was measured with 24 scans before each acquisition, while samples were investigated using 48 scans at 4 cm^{-1} resolution. Data were processed with OMNIC Specta 2.1.175 and ORIGIN 2018 software.

2.4. µ-Raman Spectroscopy

µ-Raman spectroscopy was performed on all samples using a DXRTM3 Thermo Scientific Raman Microscope coupled with a 785 nm excitation laser. The Raman spectra were collected in the 3300–100 cm^{-1} spectral range, with 5 cm^{-1} resolution, 20 to 100 scans. OMNIC Specta software managed the acquisition and elaboration of the spectra.

2.5. SEM-EDS

Sample MM.I.02219 was embedded in resin and analyzed with a Scanning Electron Microscope (SEM) Jeol JSM-5600LV coupled with Electron Dispersive Spectrometer (EDS) Oxford Instruments ISIS Series 300, with a resolution of 133 eV @ MnKα (5.9 keV). Secondary and back-scattered electron images were acquired, and EDS was used to perform both punctual analyses and mapping of the selected significant elements (Co, Al, Sn, Pb, and Na) in the samples. Isis SEMQuant software managed EDS spectra acquisitions, which were then elaborated on with Origin8.5.

2.6. GC-MS

The methodology adopted for the analysis of the organic fraction from paint tubes is the one proposed by Izzo [6] and in further developments [17–21].

An aliquot of approximately 0.3 mg was collected from the samples and put in microvials with 10 µL of Nonadecanoic acid (C19) internal standard and 30 µL of MethPrepII™ derivatization agent and left overnight to derivatize. After 24 h at room temperature, GC-MS analysis was performed by using a Thermo Scientific™ TRACETM 1300 Series GC System equipped ISQ 7000 MS with a quadrupole analyzer from Thermo Fisher Scientific (Waltham, MA, USA). Then, 1 µL of the derivatized samples was auto-injected in splitless mode at 280 °C and GC separation was performed on a fused silica capillary column DB–5MS Column (30 m length, 0.25 mm, 0.25 µm—5% phenyl methyl polysiloxane), using helium as the carrier gas (1 mL/min flow rate). The inlet temperature was 280 °C, and the MS interface was at 280 °C. The transfer line was at 280 °C and the MS source temperature was 300 °C. The temperature was programmed from 80 °C to 315 °C with a ramp of 10 °C, and held isothermally for 2 min. MS scans were performed in full-scan mode, considering the range from 40 to 650 m/z, with 1.9 scans/s. The MS Electron Ionisation energy was 70 eV.

Qualitative and quantitative analyses were performed. The analytical results of the GC-MS procedure were expressed in terms of molar ratios (P/S, A/P, %D, A/Sub, O/S). The presence of specific fatty acids (markers) was assessed through the NIST library, and using a specific library created at Ca' Foscari University for XIX–XX century commercial oil paints [19,21–24].

3. Results

3.1. Paint Surface Observations in Two Paintings

A Hirox 3D digital microscope was used to investigate the condition and appearance of the paint surface, in order to assess the different degradation phenomena and their progression in Ultramarine blue areas of the two paintings under investigation (Figures 2 and 4). The darkening appears to expand in a homogeneous way, affecting the surface of the

paint strokes while leaving the color beneath unaffected, forming a "skin-like" darkened layer atop. Darkened areas exhibit poor adhesion to the underlaying layer, with wet and waxy appearance between the cracks, dirt built up around the brushstrokes, and solvent sensitivity (Figures 2 and 4).

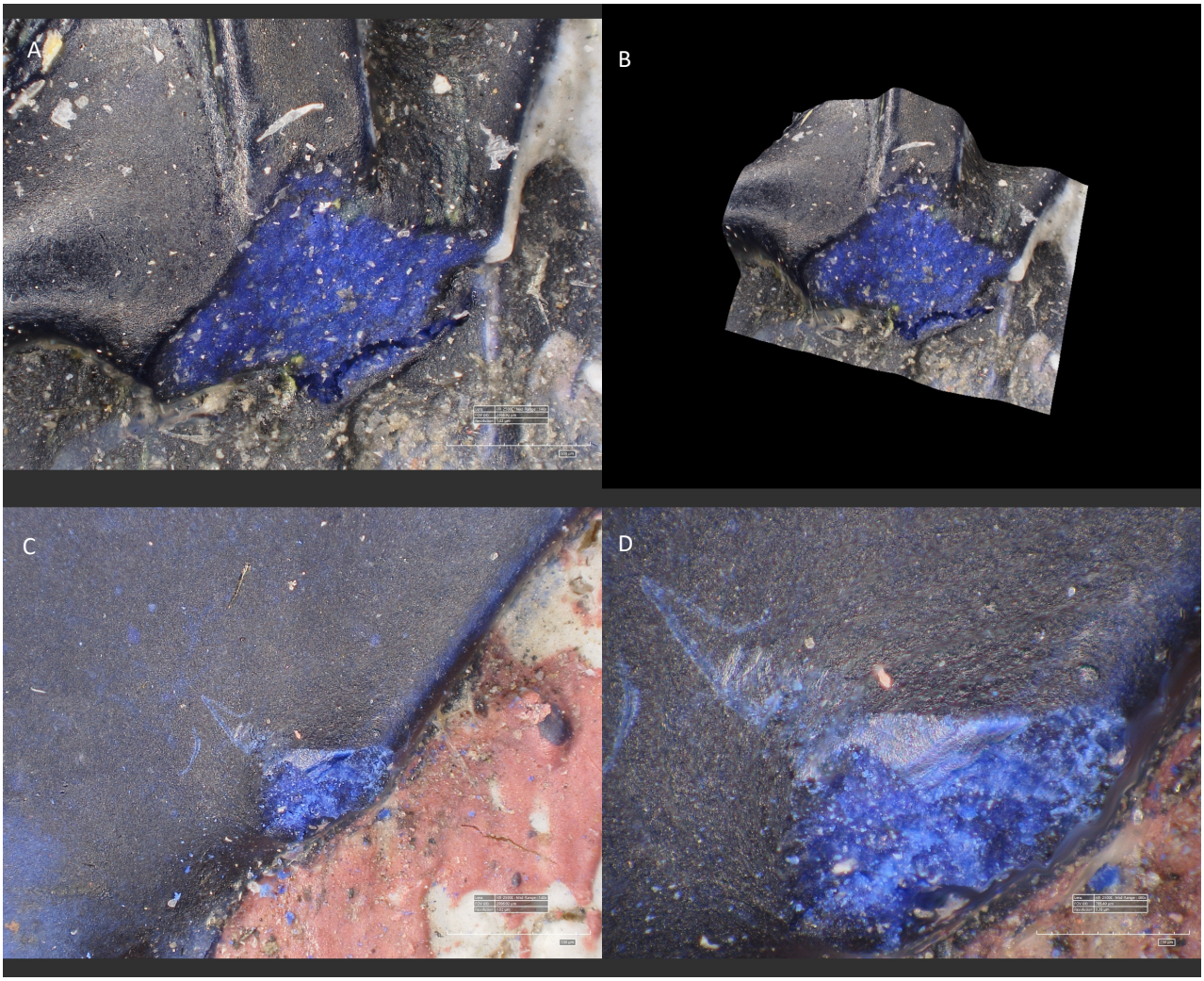

Figure 4. Hirox images of investigated areas of the two paintings, showing the darkening of the superficial layer of the brushstrokes. (**A**) Detail from the legs of the drowned boy in *The Drowned Boy* (1907–1908), 140× magnification; (**B**) 3D image of detail represented on (**A**); (**C**,**D**) details from the blue figure in the background of *Old Man in Warnemünde*, 140× and 400× magnification.

3.2. Micro-Invasive Analyses

In Tables 2 and 3, a summary of the analytical results obtained from all analyzed samples is given.

Table 2. Summary of results for inorganic compounds.

ID Tube	Analytical Results	Pigments and Other Inorganic Compounds
MM.I.01638—Ambor	ATR-FTIR: 980 cm^{-1}, 3699 cm^{-1}, 3619 cm^{-1}, 1098 cm^{-1}, 629 cm^{-1}, 1404 cm^{-1}, 1086 cm^{-1}, 871 cm^{-1} Raman: 1088 cm^{-1}, 547 cm^{-1}, 280 cm^{-1}, 252 cm^{-1}	Ultramarine blue, Calcium carbonate, kaolinite
MM.I.01632—Ambor	ATR-FTIR: 980 cm^{-1}, 1404 cm^{-1}, 1086 cm^{-1}, 871 cm^{-1} Raman: 547 cm^{-1}, 252 cm^{-1}, 401 cm^{-1}, 217 cm^{-1}	Ultramarine blue, sulphates, calcium carbonate, Fe oxides?

Table 2. *Cont.*

ID Tube	Analytical Results	Pigments and Other Inorganic Compounds
MM.I.01959—Blockx Fils	ATR-FTIR: 980 cm^{-1}, 1404 cm^{-1}, 1086 cm^{-1}, 871 cm^{-1} Raman: 547 cm^{-1}, 252 cm^{-1}	Ultramarine blue, Calcium carbonate
MM.I.02126—Lefranc	ATR-FTIR: 980 $cm^{-1,}$ 1480 cm^{-1}, 1421 cm^{-1}, 884 cm^{-1}, 854 cm^{-1}, 800 cm^{-1} Raman: 547 cm^{-1}, 252 cm^{-1}	Ultramarine blue, Mg carbonate
MM.I.02330—Vilhem Pacht	ATR-FTIR: 980 $cm^{-1,}$ 1620 cm^{-1}, 1370 cm^{-1}, 1315 cm^{-1}, 370 cm^{-1} Raman: 547 cm^{-1}, 252 cm^{-1}	Ultramarine blue, Zn white, Zn oxalates
MM.I.02219—Mussini	ATR-FTIR: 980 cm^{-1} Raman: 547 cm^{-1}, 252 cm^{-1} SEM-EDS: Pb, Si, Al, Na, C, O	Ultramarine blue, Lead white
MM.I.02424—Winsor & Newton	ATR-FTIR: 2080 cm^{-1}, 1611 cm^{-1}, 1480 cm^{-1}, 1421 cm^{-1}, 884 cm^{-1}, 854 cm^{-1}, 800 cm^{-1} Raman: 2150 cm^{-1}, 2120 cm^{-1}	Prussian blue, Carbon, Mg carbonate
MM.I.02384—Winsor & Newton	ATR-FTIR: 980 cm^{-1}, 1480 cm^{-1}, 1421 cm^{-1}, 884 cm^{-1}, 854 cm^{-1}, 800 cm^{-1} Raman: 547 cm^{-1}, 252 cm^{-1}	Ultramarine blue, Mg carbonate
MM.I.02354—Winsor & Newton	ATR-FTIR: 980 cm^{-1}, 1480 cm^{-1}, 1421 cm^{-1}, 884 cm^{-1}, 854 cm^{-1}, 800 cm^{-1} Raman: 547 cm^{-1}, 252 cm^{-1}	Ultramarine blue, Mg carbonate
MM.I.02387—Winsor & Newton	ATR-FTIR: 980 cm^{-1}, 1480 cm^{-1}, 1421 cm^{-1}, 884 cm^{-1}, 854 cm^{-1}, 800 cm^{-1} Raman: 547 cm^{-1}, 252 cm^{-1}	Ultramarine blue, Mg carbonate

Table 3. Summary of results for organic compounds. For more detail on the GC-MS results, see Section 3.4 Tables 4 and 5 and the Discussion.

ID Tube	Analytical Results	Binding Admixtures and Other Organic Compounds
MM.I.01638—Ambor	ATR-FTIR: 2925 cm^{-1}, 2855–2850 cm^{-1}, 1740 cm^{-1}, 1710 cm^{-1}, 1625 cm^{-1}, 1460 cm^{-1}, 1410–15 cm^{-1}, 1242 cm^{-1}, 1165–60 cm^{-1} Raman: 3100–3000 cm^{-1}, 3000–2800 cm^{-1}, 2885–2880 cm^{-1}, 2855–2850 cm^{-1}, 1720 cm^{-1}, 1690 cm^{-1}, 1660 cm^{-1}, 1610–1600 cm^{-1}, 1440–30 cm^{-1}, 1380 cm^{-1}, ~1300 cm^{-1}, 1296 cm^{-1}, 1136 cm^{-1}, 1065–60 cm^{-1}, 1549 cm^{-1}, 1529 cm^{-1}, 1457 cm^{-1}, 1409 cm^{-1}, 1397 cm^{-1} GC-MS: tetradehydroabietic, 7-methoxy-	Safflower/sunflower oil, Pinaceae resin, free fatty acids, Zn oleate
MM.I.01632—Ambor	ATR-FTIR: oil as above Raman: oil as above, 1458 cm^{-1}, 1439 cm^{-1} GC-MS: tetradehydroabietic, 7-methoxy-, margaric, pentadecanoiic acid	Sunflower oil + castor oil + fish liver oil? Pinaceae resin, Animal fats, levulinic acid, metal soaps
MM.I.01959—Blockx Fils	ATR-FTIR: oil as above Raman: oil as above GC-MS: Aleuritic acid	Safflower oil?, Shellac resin, Free fatty acids
MM.I.02126—Lefranc	ATR-FTIR: oil as above Raman: oil as above GC-MS: Lignoceric, behenic, levulinic acids	Peanut oil + Sunflower oil?, Levulinic acid
MM.I.02330—Vilhem Pacht	ATR-FTIR: oil as above Raman: oil as above GC-MS: levulinic, margaric, aleuritic acids	Sunflower/peanut oil?, Shellac resin, levulinic acid, margaric acid
MM.I.02219—Mussini	ATR-FTIR: oil as above Raman: oil as above, 1460 cm^{-1}, 1441 cm^{-1}, 1416 cm^{-1}, 1297 cm^{-1}, 1129 cm^{-1}, 1101 cm^{-1}, 1063 cm^{-1} SEM-EDS: Pb, Si, Al, Na, C, O GC-MS: tetradehydroabietic, 7-methoxy-, margaric, pentadecanoic, behenic, lignoceric, cerotic, melissic acids	Sunflower oil + Peanut oil, Animal fats, Pinaceae resin, Levulinic acid, Lead soaps, (Lead palmitate)

Table 3. *Cont.*

ID Tube	Analytical Results	Binding Admixtures and Other Organic Compounds
MM.I.02424—Winsor & Newton	ATR-FTIR: oil as above Raman: oil as above GC-MS: tetradehydroabietic, 7-methoxy-, behenic, lignoceric, erucic, cerotic, melissic acids	Oil + Peanut oil, Animal fats, Pinaceae resin, beeswax
MM.I.02384—Winsor & Newton	ATR-FTIR: oil as above, ~1500 cm^{-1} Raman: oil as above, 1430 cm^{-1}, ~1290 cm^{-1}, ~1130 cm^{-1}, ~1060 cm^{-1} GC-MS: Aleuritic, margaric, pentadecanoic acids	Sunflower oil?, Shellac resin, Animal fats, metal soaps
MM.I.02354—Winsor & Newton	ATR-FTIR: oil as above Raman: oil as above GC-MS: margaric, pentadecanoic. Aleuritic, levulinic acids	Sunflower oil, Animal fats, Shellac resin, Levulinic acid, metal soaps
MM.I.02387—Winsor & Newton	ATR-FTIR: oil as above, ~1500 cm^{-1} Raman: oil as above, 1430 cm^{-1}, ~1290 cm^{-1}, ~1130 cm^{-1}, ~1060 cm^{-1} GC-MS: behenic, lignoceric, margaric, pentadecanoic, levulinic acids	Oil + Peanut oil, Animal fats, Levulinic acid, metal soaps

ATR-FTIR and μ-Raman analyses were performed on all samples, providing relevant information on both the organic and inorganic fractions of the paint formulations. Moreover, μ-Raman spectroscopy was carried out to investigate if it was possible to identify differences in the spectra of different areas in the samples, pointing out the differences in composition between micro-areas of the samples. From the data acquired, it was possible to assess the main similarities between the samples and attribute them to the major components present in the paint formulations and discuss the differences.

It is possible to say, with few exceptions, that the samples are mainly composed of a lipidic binder in which the Ultramarine blue pigment is dispersed. The presence of a drying oil is confirmed both by ATR-FTIR and μ-Raman thanks to the presence of the typical absorptions at 2925 cm^{-1}, 2855–2850 cm^{-1}, 1740 cm^{-1}, 1710 cm^{-1}, 1625 cm^{-1}, 1460 cm^{-1}, 1410–15 cm^{-1}, 1242 cm^{-1} and 1165–60 cm^{-1} for ATR-FTIR and at 3100–3000 cm^{-1}, 3000–2800 cm^{-1}, 2885–2880 cm^{-1}, 2855–2850 cm^{-1}, 1720 cm^{-1}, 1690 cm^{-1}, 1660 cm^{-1}, 1610–1600 cm^{-1}, 1440–30 cm^{-1}, 1380 cm^{-1}, ~1300 cm^{-1}, 1296 cm^{-1}, 1136 cm^{-1}, and 1065–60 cm^{-1} for μ-Raman [24–26].

Ultramarine pigment was detected by its characteristic peaks at 980 cm^{-1} in ATR-FTIR spectra and at 547 cm^{-1} and 252 cm^{-1} in μ-Raman spectra [9,27]. Sample MM.I.02424 represents an exception, exhibiting the characteristic peak of Prussian Blue in both ATR-FTIR and μ-Raman at, respectively, ~2080 cm^{-1} (CN stretching) and 1611 cm^{-1}, and at ~2150 cm^{-1} and 2120 cm^{-1}.

Both ATR-FTIR spectra and μ-Raman suggest the presence of metal soaps in samples MM.I.01632, MM.I.01638, MM.I.02219, MM.I.02384, MM.I.02387, and MM.I.02354 (Figure 5). The presence of metal soaps was indicated by the detection of characteristic bands in the regions around ~1500 cm^{-1} in ATR-FTIR and ~1430 cm^{-1}, ~1290 cm^{-1}, ~1130 cm^{-1}, and ~1060 cm^{-1} in μ-Raman [25] (Figure 5). Specifically, zinc oleate has been identified in sample MM.I.01638 thanks to the detection of bands at 1549 cm^{-1}, 1529 cm^{-1} ($\upsilon_a COO^-$), 1457 cm^{-1} (δCH_2), 1409 cm^{-1}, and 1397 cm^{-1} ($\upsilon_s COO^-$) in the ATR-FTIR spectrum [26]. Metal soaps' characteristic bands around 1458 cm^{-1} and 1439 cm^{-1} were identified in Raman spectra of sample MM.I.01632 corresponding to a whitish grain, while lead palmitate was detected in Raman spectra of sample MM.I.02219 (1460 cm^{-1}, 1441 cm^{-1}, 1416 cm^{-1}, 1297 cm^{-1}, 1129 cm^{-1}, 1101 cm^{-1}, and 1063 cm^{-1}) [25].

Table 4. Qualitative results for GC-MS analysis by brand. Fatty acids and other compounds are presented in their methyl ester form, as a result of the preparation method adopted.

	Detected Compound	AMBOR		BLOCKX FILS	LEFRANC	VILH. PACHT	MUSSINI	WINSOR & NEWTON			
		MM.I.01638	MM.I.01632	MM.I.01959	MM.I.02126	MM.I.02330	MM.I.02219	MM.I.02424	MM.02384	MM.I.02354	MM.I.02387
Compounds detected	Pimelic acid, methyl ester	v	v		v		v	v	v	v	v
	Levulinic acid, methyl ester	v			v	v				v	v
	Octanoic acid, 8-hydroxy-, methyl ester				v				v	v	v
	Decanoic acid, 9-oxo-ME	v	v					v	v		
	Caprylic acid, methyl ester							v	v		
	8-Methoxytetradecanoic acid		v	v	v		v		v		v
	Undecanedioic acid, 4-oxo-, dimethyl ester	v					v		v		v
	Butanoic acid, methyl ester	v	v		v	v	v	v	v	v	v
	Pentadecanoic acid, methyl ester		v			v	v	v	v	v	v
	Palmitoleic acid, methyl ester		v		v	v	v	v	v	v	v
	Aleuritic acid, methyl ester, trimethyl eter	v		v		v	v		v	v	
	3-Oxo-1,8-octanedicarboxylic acid, dimethyl ester	v	v	v		v	v	v		v	v
	Margaric acid, methyl ester		v			v	v	v	v	v	v
	Octadecanoic acid, 9,10-epoxy-, methyl ester	v	v		v	v		v		v	v
	Octadecanoic acid, 10-oxo-, methyl ester	v	v	v	v	v	v	v			v
	Octadecanoic acid, 9,10-dihydroxy-, methyl ester	v	v	v	v	v	v	v	v	v	v
	Tetradehydroabietic, 7-methoxy-, methyl ester	v	v				v	v			
	Eicosane, methyl ester										
	Ethyl stearate, 9,12-diepoxy					v					
	Erucic acid,methyl ester							v			
	Behenic acid, methyl ester				v	v	v	v	v	v	v
	Methyl Ricinoleate	v									
	Heptacosane, methyl ester										
	Lignoceric acid, methyl ester				v	v	v	v			v
	Hexacosanoic, methyl ester				v						
	Docosane, methyl ester										
	Cerotic acid, methyl ester						v	v			
	Hentriacontane, methyl ester										
	Melissic acid, methyl ester						v				

Table 5. Quantitative results for GC-MS analysis. Fatty acids and other compounds are presented in their methyl ester form, as a result of the preparation method adopted. Fatty acid presence is reported as a percentage (%).

	Detected Compound	AMBOR		BLOCKX FILS	LEFRANC	VILH. PACHT	MUSSINI	WINSOR & NEWTON			
		MM.I.01638	MM.I.01632	MM.I.01959	MM.I.02126	MM.I.02330	MM.I.02219	MM.I.02424	MM.02384	MM.I.02354	MM.I.02387
Fatty acids (W%)	Suberic acid, methyl ester	11.22	17.80	13.44	5.77	5.88	15.31	6.01	10.54	5.14	7.94
	Azelaic acid, methyl ester	29.57	39.76	31.61	24.67	17.85	32.47	14.76	34.11	22.16	20.10
	Sebacic acid, methyl ester	4.24	7.08	4.60	1.56	1.62	4.00	2.61	5.34	1.79	2.60
	Myristic acid, methyl ester	1.11	1.37	1.47	1.62	1.59	1.85	1.13	1.66	1.42	1.49
	Palmitic acid, methyl ester	15.52	13.53	19.97	26.13	27.40	25.78	18.61	16.84	22.76	34.87
	Oleic acid, methyl ester	13.43	7.48	3.53	18.29	21.78	1.05	27.81	3.82	21.09	7.21
	Stearic acid,methyl ester	6.16	6.09	8.44	11.52	12.82	11.73	17.91	14.78	11.38	19.09
	Linoleic acid, methyl ester	1.43	0.82	-	0.93	0.03	0.13	1.98	0.09	0.30	0.97
	Linolenic acid, methyl ester	1.02	0.90	-	-	-	0.33	0.18	-	0.24	0.12
	Glycerol	16.29	5.16	16.93	9.51	11.02	7.35	9.00	12.82	13.71	5.60
Molar ratios among fatty acids	A/P	1.91	2.94	1.58	0.94	0.65	1.26	0.79	2.03	0.97	0.58
	P/S	2.52	2.22	2.37	2.27	2.14	2.20	1.04	1.14	2.00	1.83
	%D	45.03	64.65	49.65	32.00	25.36	51.78	23.39	49.99	29.09	30.64
	O/S	2.18	1.23	0.42	1.59	1.70	0.09	1.55	0.26	1.85	0.38
	A/Sub	2.64	2.23	2.35	4.28	3.03	2.12	2.46	3.24	4.31	2.53

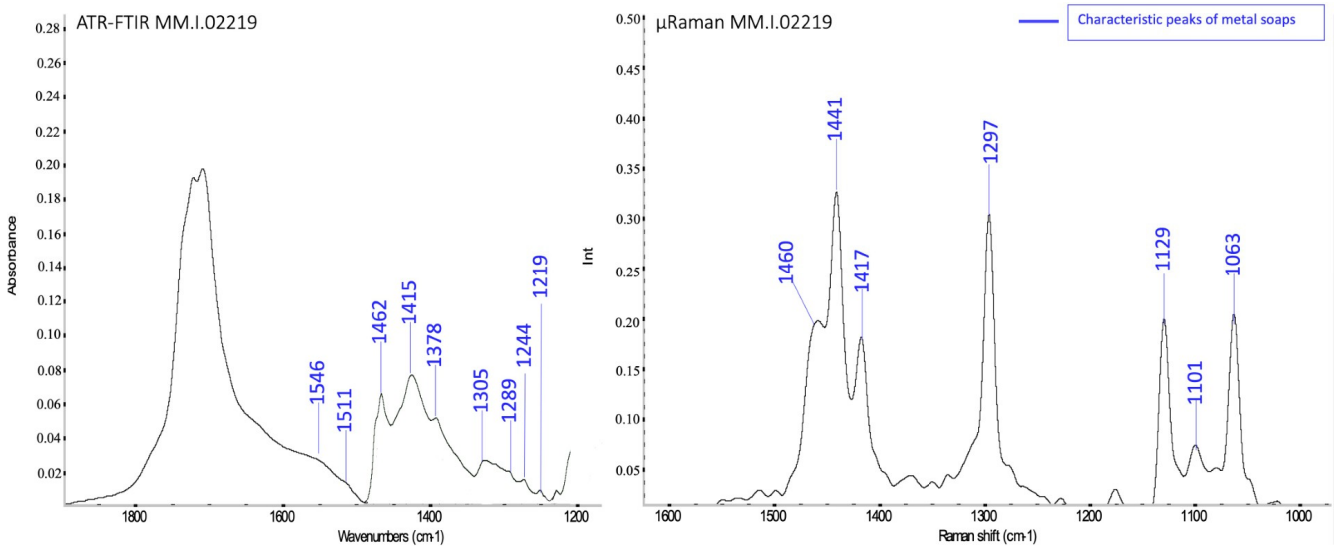

Figure 5. ATR-FTIR (**left**) and μ-Raman spectra (**right**) of sample MM.I.02219 showing peaks attributed to the presence of metal soaps.

The presence of kaolinite was found in sample MM.I.01638 thanks to bands at 3699 cm^{-1} (υAl≡O–H), 3619 cm^{-1} (υOH), 1098 cm^{-1} (υSi–O–Si), and 692 cm^{-1} (υAl–O–H) in the ATR-FTIR spectrum. Its presence could be associated with either its use as an extender or as a residue from the Ultramarine Blue pigment. Chalk was retrieved in samples MM.I.01638 and MM.I.01959 in Raman spectra (280 cm^{-1} and 1088 cm^{-1}) [28].

Magnesium carbonate and hydromagnesite have been identified in ATR-FTIR spectra of samples MM.I.02126, MM.I.02424, MM.I.02354, MM.I.02384, and MM.I.02387, thanks to the characteristic sharp peaks at ~1480 cm^{-1} and 1421 cm^{-1} (CO_3^{2-}/HCO_3^- asymmetric stretching), 884 cm^{-1} (υ carbonate), 854 cm^{-1} (υ carbonate), and 800 cm^{-1} (CO_3^{2-} bending vibrations) [29,30].

The presence of oxalates has been established by the detection of bands at around 1620 cm^{-1}, ~1370 cm^{-1}, and ~1315 cm^{-1} in ATR-FTIR spectra of samples MM.I.02126 and MM.I.02330. Specifically, Zn oxalate has been hypothesized for sample MM.I.02330 (1619 cm^{-1}, ~1370 cm^{-1}, and 1317 cm^{-1}) [31], consistent with the detection of ZnO in the same sample (peaks around ~400 cm^{-1}) [29].

Raman spectroscopy of sample MM.I.01632 revealed the presence of iron oxides corresponding to a black grain (401 cm^{-1} and 217 cm^{-1}) [28].

Sample MM.I.02384 spectra presented a series of peaks of difficult attribution (492 cm^{-1}, 366 cm^{-1}, 181 cm^{-1}, and 148 cm^{-1}).

Significantly, the μ-Raman spectra of sample MM.I.02424 showed distinct indications of the existence of inorganic carbon. This was identified thanks to the presence of distinctive broad bands observed at approximately 1560 cm^{-1} and 1340 cm^{-1} in two specific regions of the samples [28].

3.3. SEM-EDS

Sample MM.I.02219 was investigated with SEM-EDS (Figure 6).

The presence of a grain of whitish material in sample MM.I.02219 was observed, and EDS spectra confirmed it to be mainly composed of lead (Figure 6). The spectrum of point c, instead, corresponding to a dark blue area, registered the presence of Al, Na, and Si, which are the main elements in Ultramarine blue pigment. Furthermore, the detection of a relatively intense peak corresponding to carbon on spectrum b, together with the lower atomic brightness of the region and the typical granular structure of the area, confirm the formation of lead soaps as described by Izzo et al., 2021 [29].

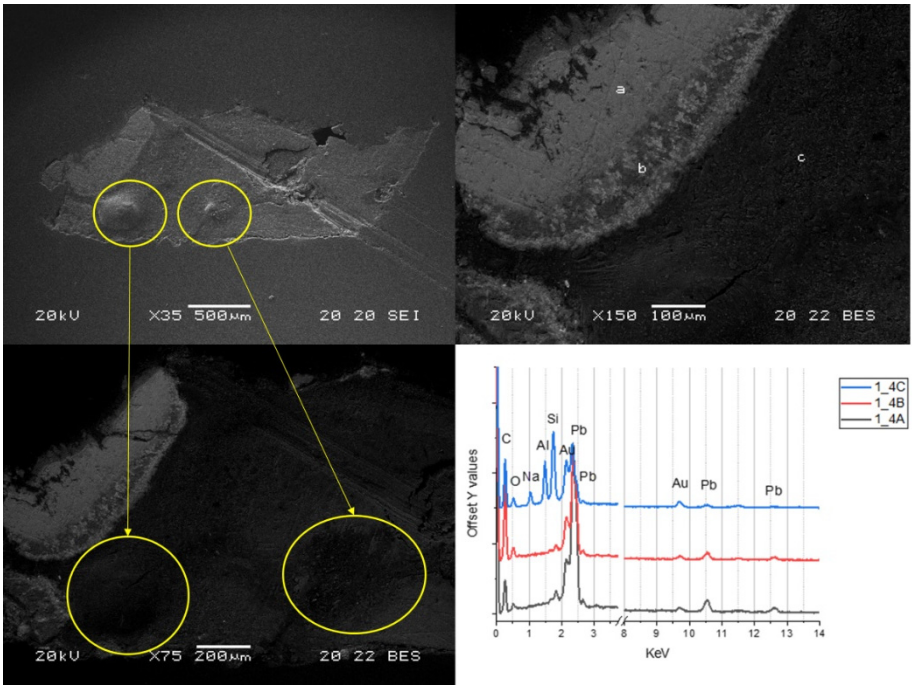

Figure 6. SEM-EDS results for sample MM.I.02219. Top right, secondary electrons image taken at 35×; bottom right, back-scattered electrons image taken at 75×, in the yellow circle; medium separation is highlighted. Top left, back-scattered image taken at 150× indicating the area on which Energy Dispersive Spectroscopy was performed (spectra a, b, c); bottom left, EDS spectra of points a, b, c.

From the comparison between the secondary electron and the backscattered electron images in Figure 6, the presence of an almost spherical, bubble-like region characterized by an enrichment of the organic fraction is clear in the left lower side of the sample, as it can be deduced by the lower brightness of the area compared to the BES image. The same comparison makes evident the presence of lead white in correspondence with the white area, due to the higher brightness in the BES image.

3.4. GC-MS

In general, the chromatographic analysis revealed the presence of typical fatty acids commonly found in cured drying oils. These include various types such as short-chain fatty acids, dicarboxylic acids (like pimelic, suberic, azelaic, and sebacic acids), as well as saturated long-chain fatty acids (such as myristic, palmitic, stearic, arachidic, and behenic acids). Additionally, unsaturated fatty acids, particularly oleic acid, were detected. The analysis also identified peaks associated with glycerol derivatives, according to the derivatization process. Furthermore, a significant presence of oxidized octadecanoic acids (including oxo-, hydroxy-, and methoxy-octadecanoic acids) was noted, indicating their formation through the oxidative breakdown of originally present unsaturated fatty acids in the fresh formulations [6,17–19,21,23,32].

Dicarboxylic acids like azelaic, suberic, and sebacic acids were detected, since they represent the main products of oxidative degradation and are generated as a result of the breakdown of triglycerides within the cross-linked network [6,17–19,21,23,32].

The %D, A/P, and O/S molar ratios can provide an important overview of the degree of oxidation reached by the different samples [6,17–19,21,23,32]. It is important to highlight that the condition and appearance of the paint tubes samples were different, ranging from completely dried out samples to tacky, still liquid, and spreadable ones.

The ratios of azelaic to suberic acid (A/Sub) were also calculated for all the samples and interestingly displayed values consistent with pre-heated oils as reported in the literature, ranging between 2.5 and 3 for many samples.

Although the identification of the kind of vegetable oil is difficult to achieve for modern and contemporary oil paints when only considering the P/S ratios [6,18–20,22,24], some hypotheses can be formed by considering these ratios and the presence of peculiar fatty acids, taking into account both the molar ratios and the detection of specific markers in some samples.

In addition to linseed oil, safflower/sunflower oil, castor oil, and peanut oil were hypothesized to be present in most samples (MM.I.02354, MM.I.02387, MM.I.02424, MM.I.02330, MM.I.02219, MM.I.02126, MM.I.01632, and MM.I.01638) thanks to the identification of their specific markers (Figure 7). Tables 3 and 4 summarize the results obtained regarding the organic fraction of the paints under investigation.

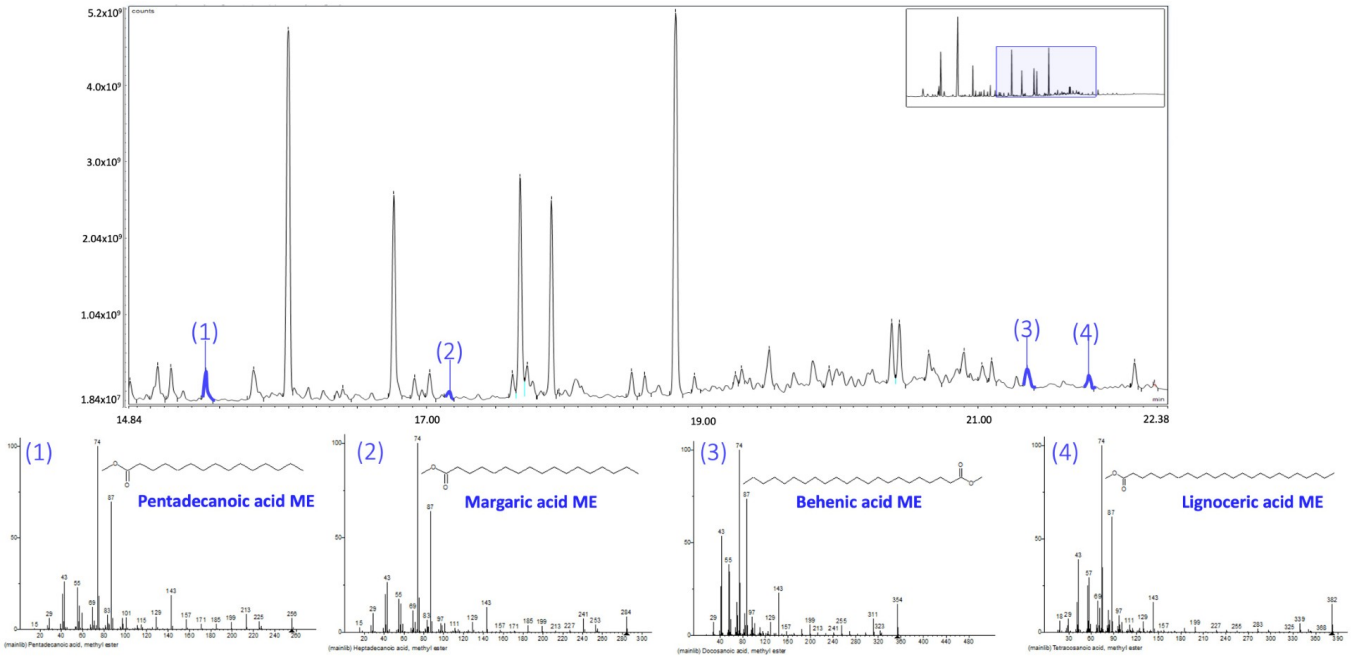

Figure 7. Chromatogram of sample MM.I.01632 by Ambor. Relevant peaks concerning the presence of Pentadecanoic, Margaric, Behenic, and Lignoceric acids' methyl esters are highlighted, and their mass spectra reported.

Levulinic acid was detected in some samples (MM.I.01632, MM.I.02126, MM.I.02330, MM.I.02354, and MM.I.02387): its use might be associated with preservative purposes.

Based on the results obtained from both qualitative and quantitative analyses, the binding admixtures proposed in Table 3 were assessed according to the literature [6,33–36].

Moreover, the presence of significative compounds pointing to minor additions of other materials besides siccative oils has been assessed for almost all samples. Specifically, aleuritic acid was identified in samples MM.I.01959, MM.I.02219, MM.I.02330, MM.I.02384, and MM.I.02354, opening the possibility of the use of shellac resin in the binding mixture, this being one of the main aliphatic components of shellac resin [34] (Mills and White, 1994). Other resinaceous materials, in particular from the family of *Pinaceae resins*, have been identified in samples MM.I.02424, MM.I.02219, M.I.01632, and MM.I.01638 thanks to the presence of at least one of the specific markers for this class of resins (dehydroabietic acid, tetradehydroabietic, 7-methoxy-, 7-oxodehydroabietic acid) [34].

Margaric and pentadecanoic acids have been identified in samples MM.I.01632 (Figure 7), MM.I.02424, MM.I.02384, MM.I.02387, and MM.I.02354, pointing to the presence of animal fat or other animal-originated compounds in these paints [36]. Moreover, thiophenecarboxylic acid, a specific marker for fish glue, has been identified in sample MM.I.01632.

Beeswax was identified in samples MM.I.02219 and MM.I.02424 thanks to the presence of long-chain fatty acids (lignoceric acid, melissic acid, cerotic acid, hexacosanoic acid) and a series of odd-numbered alkanes [34].

4. Discussion

4.1. Characterization of Pigments, Binding Media, and Additives Present in Industrial Paint Tubes

In the present study, ten paint tubes labeled as Ultramarine blue oil paint made by six different brands were analyzed, aiming to uncover some of the characteristics of the early 20th century industrial oil paints used by Edvard Munch.

The description reported on the original paint tube labels rarely reflects the complexity in the composition of the paints inside them.

Apart from the use of drying oils other than the traditional linseed oil (for example, sunflower or safflower oil as a substitute for it), it was possible to prove the use of several semi- or non-drying oils, including castor seed oil and peanut oil, used as adulterants. In fact, peanut oil was identified within the Mussini Ölfarben Schmincke, as well as in two of the paint tubes by Winsor & Newton. This brings to light numerous conservation issues that must be addressed when preserving artworks that could contain these oils, as has been discussed in previous studies [21]. Given that a substantial portion of the paint tubes in the MUNCH museum collection consist of Winsor & Newton products, it is reasonable to assume that artworks in the museum may have been created using paints from this brand.

Moreover, in the samples from the paint tubes by the same brand, as well as in some of the ones by Ambor and Mussini Ölfarben Schmincke, the presence of animal fats has been identified. This result is again in accordance with the literature regarding Winsor & Newton [37], but represents a new finding for Mussini Ölfarben Schmincke and the less-known Ambor brand.

Furthermore, the presence of $MgCO_3$ has been found in all Ultramarine blue paints by Winsor & Newton, once again in accordance with the literature [37]. The same additive, which has been found to be related to the water sensitivity of modern paintings, was also found in the Ultramarine blue paint sample from the French brand LeFranc.

The detection of aleuritic acid, attributed to the presence of shellac resin [34,38] in a vast number of samples from different brands, highlights the use of this additive in paint formulations. Additionally, either together with or in place of shellac resin, the identification of terpenic compounds form the *Pinaceae* family in many samples, confirming the addition of these materials as common practice in the manufacture of early 20th century oil paints, most likely as thickeners.

Another additive vastly implied in the paint formulations analyzed and worth mentioning is levulinic acid. Samples from Ambor, Lefranc, Mussini Ölfarben Schmincke, Vilhem Pacht, and Winsor & Newton showed the presence of this additive. Its use in paint formulations was mainly as a preservation agent, preventing microbial growth and prolonging shelf-life [39].

Margaric acid was found as a free fatty acid in Vilhem Pacht paints, probably used as an additive to improve the consistency and rheological characteristics of the paint [21,37].

The use of waxy materials (such as beeswax) as stabilizers—both for rheological purposes, to impart the right consistency, and to keep the pigment in suspension [6,21]—has been found in Winsor & Newton and in Mussini Ölfarben Schmincke tube samples.

GC-MS analyses, even if the protocol used was specifically aimed at analyzing the lipidic fraction, allowed the identification of the presence of proteinaceous materials (as methyl esters) in an Ultramarine blue paint by Ambor.

Since the ATR-FTIR spectrum for this sample does not provide evidence of the presence of proteins, it is likely that their quantities were below the detection limit for this technique, that is, 5% in weight. Specifically, a marker for fish glue was found in combination with animal fats. Even if we cannot exactly date the paint tubes analyzed, we know that the paint tubes collection owned by the MUNCH Museum covers a span of approximately sixty years between the late 19th and early 20th century [4], in which the raw materials shortage for paint production during WWI had to be considered. Recently, Wedvik [40] reconstructed the main surrogates for linseed oil during that time in Norway, pointing out that fish liver and whale oil were possibly utilized in local paint production. Even if *Ambor* was produced

by a French manufacturer, we believe that this finding and interesting consideration should be taken into account, since this manufacturer was also active during WWI.

The complexity of this paint—containing proteinaceous materials, resins, animal fats, and waxes together with vegetable oils—point towards a mixture that can hardly be identified as simply "oil" paint tubes, as was reported on the tubes' labels.

A few inorganic extenders have also been identified in the analyzed samples.

The composition of Ambor and Blockx Fils Ultramarine blue paints was shown to include $CaCO_3$ and kaolinite.

Zinc oxide has been found in Vilhem Pacht Ultramarine blue paint, possibly to impart a lighter shade to the paint. Pb white was instead found in the Mussini Ölfarben Schmincke samples, as previously discussed (sample MM.I.02219).

Zinc soaps have been found in Ultramarine blue by Ambor that did not show the presence of ZnO or any other source of Zn cations, therefore suggesting the deliberate addition of such components to paint formulations. In fact, metal carboxylates have commonly been used as dispersion agents in oil paint formulations since the early 20th century [6,21,33,41]. Nonetheless, the presence of Zn soaps, either as paint additives or secondary products resulting from the interaction between the oil medium and the inorganic fraction, have been found to be the cause of different degradation patterns [42].

Finally, Prussian blue has been found to be used instead of Ultramarine blue pigment in a paint tube by Winsor & Newton labeled as "Deep Ultramarine" (sample MM.I.02424), highlighting the discrepancy often encountered between labels and the actual composition of commercial products. It is in fact important to remember that the labeling of the color on paint tubes often refers to the appearance and tone of the paint rather than the chemical composition.

4.2. Considerations on the Darkening Observed in Paintings in Relation to the Composition of Paint Tubes from Munch's Collection

The results of the recent study suggest the presence of metal soaps in the paints' formulations, along with the presence of semi- and non-drying oils. The distinctive degradation of Ultramarine blue paints, resulting in a darkened, skin-like layer observed in the paintings, might be a degradation pattern due to the excess of metal soaps in the paint formulations.

This hypothesis pertains to the development of an enriched medium exudate atop the pristine color due to paint phase separation induced by an excess of metal soaps. This concept is consistent with the findings of Burnstock et al. [43], who proposed a similar mechanism for water-sensitive paintings, particularly noting the susceptibility of Ultramarine blue to this deterioration. Other notable studies in the literature confirm these finding, suggesting the relevance of the presence of Al and Zn stearates and slow drying oils in exacerbating these effects [32,44–47].

Furthermore, the migration of stearates to the surface could lead to increased sensitivity of the organic portion of the paint to moisture, as also suggested by Tempest et al. [46] and van den Berg [45], explaining what has been observed in paintings by Karel Appel, Jasper Johns, and Mia Tarney. It is also likely that the painting technique used in our case studies, consisting of the application of the paint directly from the tube to the canvas, would have enhanced this effect due to a non-homogeneous mixing of the paint components, as also observed in painting by Karel Appel and Alexis Mérodack-Jeaneau [47,48].

The mechanism dictating this phenomenon is yet to be fully understood, but the authors seem to agree with the hypothesis that the excess of metal stearates inhibits the cross-linking of the medium during drying [43–46]. Further studies must focus on studying the aging of these complex mixtures in controlled environment, to understand how the environmental parameters, specifically relative humidity, affect the paintings and how to mitigate these effects in the conservation practice and museum exhibitions.

In the present study, we observed a similar effect in sample MM.I.02219, an Ultramarine blue paint by Mussini Ölfarben Schmincke. In fact, comparisons between BES and SEI images from SEM analyses revealed a clear separation of the medium in different areas, as

well as the formation of lead soaps aggregates (Figure 7). Furthermore, the hypothesis that attributes the darkening effect to the organic fraction of the paint formulations seems to be in accordance with the findings by Strand-Ferrer et al. [2]. As matter of fact, the cited study did not point out any significant differences in the XANES spectra of Ultramarine blue samples of pristine and darkened areas from the *Old Man in Warnemünde* painting, indirectly supporting the hypothesis that sees the organic fraction as responsible for the skin-like darkening effect in Ultramarine blue paints.

5. Conclusions

The outcomes of this study uncover the intricate makeup of industrial oil paints used in early 20th century artworks. Beyond their importance in understanding the manufacturing practices of that period, these discoveries hold significant relevance in the conservation of Cultural Heritage, particularly in connection with the artist Edvard Munch and his painted works. Through thorough analysis, the study unveils a diverse panorama of organic and inorganic components, additives, adulterants, and unexpected compounds within the examined paint tube samples. This complexity poses a challenge for artwork preservation, emphasizing the necessity of deeper insight into paint materials beyond what is typically provided on labels or manufacturer catalogues.

A key finding of this research pertains to the varied additives present in the oil paints across different brands. These include animal fats, resins such as shellac and Pinaceae resins, levulinic acid serving as a preservative, and beeswax for consistency and stabilization. This highlights discrepancies between labeled ingredients and actual content. Additionally, the presence of magnesium carbonate, zinc oxide, and lead white further adds to the complexity of the paint's composition, aging, and behavior.

Moreover, the results suggested the key role played by metal carboxylates. The presence of zinc and lead soaps, as well as other carboxylates, in more than one paint tube from the artist's collection supports the hypothesis that these compounds were intentionally incorporated into the paint formulations rather than arising accidentally due to the interaction of the oil medium with metal cations in the paint. The present study suggests the contribution of these components, together with the use of semi- and/or non-drying oil, in triggering the medium-pigment separation, possibly causing the darkening effect observed in the paintings by Munch.

Further studies should focus on validating this hypothesis by recreating this effect in a controlled environment and through analyses on samples from paintings.

Author Contributions: B.G.B.—conceptualization, data curation, investigation, methodology, writing (original draft). E.-J.S.F.—conceptualization, writing (original draft). M.G.—investigation, methodology. L.F.—investigation. I.C.A.S.—conceptualization, resources, supervision, writing (original draft). F.C.I.—resources, fundings, supervision, methodology, writing (original draft). All authors have read and agreed to the published version of the manuscript.

Funding: This research received no external funding.

Data Availability Statement: The analytical data is available internally at MUNCH and at Ca Foscari University in Venice as part of research database. It can be consulted on request.

Acknowledgments: The kind support of the PERCEIVE project is acknowledged, via funding from the European Union's Horizon research and innovation program under grant agreement No. 101061157. Francesca Izzo acknowledges "Patto per Venezia"- Municipality of Venice for funding part of the instrumentation used for the characterization of heritage samples.

Conflicts of Interest: The authors declare no conflicts of interest.

References

1. Ferrer, J.S. Altered Blue and Red Paints: Investigations of Old Man in Warnemünde and The Drowned Boy by Edvard Munch (1863–1944). Master's Thesis, University of Oslo, Oslo, Norway, 2019.

2. Ferrer, J.S.; Sandu, I.C.A.; Cardoso, A.M.; Candeias, A.; Borca, C.N. Chapter 15: Investigating Colour Changes in Red and Blue Paints—A Preliminary Study of Art Materials and Techniques in Edvard Munch's Old Man in Warnemünde (1907). In *Conservation of Modern Oil Paintings*; van den Berg, K.J., Bonaduce, I., Burnstock, A., Ormsby, B., Scharff, M., Carlyle, L., Heydenreich, G., Keune, K., Eds.; Springer: Cham, Switzerland, 2021.
3. Sandu, I.C.A.; Ferrer, J.S.; Rosi, F.; Buti, D.; Monico, L.; Magrini, D.; Costantino, C.; Cartechini, L.; Romani, A.; Miliani, C.; et al. Colours of modernism in Edvard Munch's paintings from Warnemünde period. In Proceedings of the COLOURS 2022 Conference, Evora, Portugal, 14–16 September 2022; p. 34.
4. Sandu, I.C.A.; Sandbakken, E.G.; Ferrer, J.S.; Syversen, T.; Hull, A. The Art Historical Materials Collection at Munch: Colours, Brands, Labels. *Int. J. Conserv. Sci.* **2022**, *13*, 1653–1664.
5. Ward, G.W.R. *The Grove Encyclopedia of Materials and Techniques in Art*; Oxford University Press: Oxford, UK, 2008.
6. Izzo, F.C. 20th Century Artists' Oil Paints: A Chemical-Physical Survey. Ph.D. Thesis, Ca' Foscari University of Venice, Venice, Italy, 2010.
7. van Eikema Hommes, M. *Changing Pictures Discoloration in 15th—17th Century Oil Paintings*; Archetype Publications Ltd.: London, UK, 2004.
8. Carlyle, L. *The Artist's Assistant: Oil Painting Instruction Manuals and Handbooks in Britain, 1800–1900, with Reference to Selected 18th-Century Sources*; Archetype Publications Ltd.: London, UK, 2001; p. 608.
9. Roy, A. Ultramarine Blue, Natural and Artificial. In *Artists' Pigments: A Handbook of Their History and Characteristics*; National Gallery of Art, Washington; Archetype Publications: London, UK, 1993; Volume 2, pp. 37–67.
10. Pamer, T. 'Modern Blue Pigments' in AIC Preprints, American Institute for Conservation of Historic and Artistic Works. In Proceedings of the 6th Annual Meeting, Fort Worth, TX, USA; 1978; pp. 107–118.
11. Gettens, R.J.; Stout, G.L. *Painting Materials—A Short Encyclopaedia*; Dover Publications: New York, NY, USA, 1966.
12. de la Rie, E.R.; Michelin, A.; Ngako, M.; Del Federico, E.; Del Grosso, C. Photo-catalytic degradation of binding media of ultramarine blue containing paint layers: A new perspective on the phenomenon of "ultramarine disease" in paintings. *Polym. Degrad. Stab.* **2017**, *144*, 43–52. [CrossRef]
13. Del Federico, E.; Newman, J.; Tyne, L.; O'Hern, C.; Isolani, L.; Jerschow, A. Solid state NMR studies of ultramarine pigments discoloration. *Mat. Res. Soc. Symp. Proc.* **2006**, *984*, 0984-MM07-13. [CrossRef]
14. Del Federico, E.; Shöfberger, W.; Schelvis, J.; Kapetanaki, S.; Tyne, L.; Jerschow, A. Insight into framework destruction in ultramarine pigments. *Inorg. Chem.* **2006**, *45*, 1270–1276. [CrossRef]
15. Bayliss, S.; van den Berg, K.J.; Burnstock, A.; de Groot, S.; van Keulen, H.; Sawicka, A. An investigation into the separation and migration of oil in paintings by Erik Oldenhof. *Microchem. J.* **2016**, *124*, 974–982. [CrossRef]
16. Bronken, I.A.T.; Boon, J.J.; Corkery, R.; Steindal, C.C. Changing surface features, weeping and metal soap formation in paintings by Karel Appel and Asger Jorn from 1946–1971. *J. Cult. Herit.* **2019**, *35*, 279–287. [CrossRef]
17. Izzo, F.C.; Ferriani, B.; van den Berg, J.K.; van Keulen, H.; Zendri, E. 20th century artists' oil paints: The case of the Olii by Lucio Fontana. *J. Cult. Herit.* **2014**, *15*, 557–563. [CrossRef]
18. Caravá, S.; García, C.R.; de Agredos-Pascual, M.L.V.; Mascarós, S.M.; Izzo, F.C. Investigation of modern oil paints through a physico-chemical integrated approach. Emblematic cases from Valencia, Spain. *Spectrochim. Acta Part A Mol. Biomol. Spectrosc.* **2020**, *240*, 118633. [CrossRef]
19. Fuster-López, L.; Izzo, F.C.; Andersen, C.K.; Murray, A.; Vila, A.; Picollo, M.; Stefani, L.; Jiménez, R.; Aguado-Guardiola, E. Picasso's 1917 paint materials and their influence on the condition of four paintings. *SN Appl. Sci.* **2020**, *2*, 2159. [CrossRef]
20. Izzo, F.C.; Källbom, A.; Nevin, A. Multi-analytical assessment of bodied drying oil varnishes and their use as binders in armour paints. *Heritage* **2021**, *4*, 3402–3420. [CrossRef]
21. Izzo, F.C.; van den Berg, K.J.; van Keulen, H.; Ferriani, B.; Zendri, E. Modern Oil Paints, Formulations, Organic Additives and Degradation: Some Case Studies. In *Issue in Contemporary Oil Paint*; van den Berg, K.J., Burnstock, A., de Keijzer, M., Krueger, J., Learner, T., de Tagle, A., Heydenreich, G., Eds.; Springer International Publishing: Manhattan, NY, USA, 2014; pp. 75–104.
22. Fuster-López, L.; Izzo, F.C.; Damato, V.; Yusà-Marco, D.J.; Zendri, E. An insight into the mechanical properties of selected commercial oil and alkyd paint films containing cobalt blue. *J. Cult. Herit.* **2019**, *35*, 225–234. [CrossRef]
23. Izzo, F.C.; Zendri, E.; Biscontin, G.; Balliana, E. TG–DSC analysis applied to contemporary oil paints. *J. Therm. Anal. Calorim.* **2011**, *104*, 541–546. [CrossRef]
24. Vandenabeele, P.; Wehling, B.; Moens, L.; Edwards, H.; De Reu, M.; Van Hooydonk, G. Analysis with micro-Raman spectroscopy of natural organic binding media and varnishes used in art. *Anal. Chim. Acta* **2000**, *407*, 261–274. [CrossRef]
25. Robinet, L.; Corbeil, M.C. The Characterization of Metal Soaps. *Stud. Conserv.* **2013**, *48*, 23–40. [CrossRef]
26. Mazzeo, R.; Prati, S.; Quaranta, M.; Joseph, E.; Kendix, E.; Galeotti, M. Attenuated total reflection micro-FTIR characterization of pigment–binder interaction in reconstructed paint films. *Anal. Bioanal. Chem.* **2008**, *392*, 65–76. [CrossRef]
27. Osticioli, I.; Mendes, N.F.C.; Nevin, A.; Francisco; Gil, P.S.C.; Becucci, M.; Castellucci, E. Analysis of Natural and Artificial Ultramarine Blue Pigments Using Laser Induced Breakdown and Pulsed Raman Spectroscopy, Statistical Analysis and Light Microscopy. *Spectrochim. Acta Part A Mol. Biomol. Spectrosc.* **2009**, *73*, 525–531. [CrossRef]
28. Caggiani, M.C.; Cosentino, A.; Mangone, A. Pigments Checker version 3.0, a handy set for conservation scientists: A free online Raman spectra database. *Microchem. J.* **2016**, *129*, 123–132. [CrossRef]

29. Izzo, F.C.; Kratter, M.; Nevin, A.; Zendri, E. A Critical Review on the Analysis of Metal Soaps in Oil Paintings. *Chem. Open Rev.* **2021**, *10*, 904. [CrossRef]
30. Vahur, S.; Teearu, A.; Leito, I. ATR-FT-IR spectroscopy in the region of 550–230 cm−1 for identification of inorganic pigments. *Spectrochim. Acta Part A* **2010**, *75*, 1061–1072. [CrossRef]
31. Harrison, J.; Lee, J.; Ormsby, B.; Payne, D.J. The influence of light and relative humidity on the formation of epsomite in cadmium yellow and French ultramarine modern oil paints. *Herit. Sci.* **2021**, *9*, 107. [CrossRef]
32. Simonsen, K.P.; Poulsen, J.N.; Vanmeert, F.; Ryhl-Svendsen, M.; Bendix, J.; Sanyova, J.; Janssens, K.; Mederos-Henry, F. Formation of zinc oxalate from zinc white in various oil binding media: The influence of atmospheric carbon dioxide by reaction with $^{13}CO_2$. *Herit. Sci.* **2020**, *8*, 126. [CrossRef]
33. van den Berg, J.D.J. Analytical Chemical Studies on Traditional Oil Paints. Ph.D. Thesis, University of Amsterdam, Amsterdam, The Netherlands, 2002.
34. Mills, J.S.; White, R. *The Organic Chemistry of Museum Objects*, 2nd ed.; Butterworth-Heinemann: Oxford, UK, 1994.
35. Dubois, V.; Breton, S.; Linder, M.; Fanni, J.; Parmentier, M. Fatty acid profiles of 80 vegetables oils with regard to their nutritional potential. *Eur. J. Lipid Sci. Technol.* **2007**, *109*, 710–732. [CrossRef]
36. Carrin, M.E.; Carelli, A.A. Peanut oil: Compositional data. *Eur. J. Lipid Sci. Technol.* **2010**, *112*, 697–707. [CrossRef]
37. Banti, D.; La Nasa, J.; Tenorio, A.L.; Modugno, F.; van den Berg, J.K.; Lee, J.; Ormsby, B.; Burnstock, A.; Bonaduce, I. A molecular study of modern oil paintings: Investigating the role of dicarboxylic acids in the water sensitivity of modern oil paints. *RSC Adv.* **2018**, *8*, 6001. [CrossRef]
38. Wang, L.; Ishida, Y.; Ohtani, H.; Tsuge, S.; Nakayama, T. Characterization of Natural Resin Shellac by Reactive Pyrolysis−Gas Chromatography in the Presence of Organic Alkali. *Anal. Chem.* **1999**, *71*, 1316–1322. [CrossRef]
39. Izzo, F.C.; Conservation and Heritage Science Group, Ca' Foscari University of Venice, Venice, Italy. Personal communication, 2023.
40. Wedvik, B. A Glimpse into the House and Decorative Paint Market in Norway During World War I (1914–1918). In *Conservation of Modern Oil Paintings*; van den Berg, K.J., Bonaduce, I., Burnstock, A., Ormsby, B., Schar, M., Carlyle, L., Heydenreich, G., Keune, K., Eds.; Springer Nature Switzerland AG: Cham, Switzerland, 2019.
41. Tumosa, C.S. A brief history of aluminum stearate as a component of paint. *Waac Newsl.* **2001**, *23*, 10–11.
42. Beerse, M.; Keune, K.; Iedema, P.; Woutersen, S.; Hermans, J. Evolution of Zinc Carboxylate Species in Oil Paint Ionomers. *ACS Appl. Polym. Mater.* **2020**, *2*, 5674–5685. [CrossRef]
43. Burnstock, A.; van den Berg, K.J.; de Groot, S.; Wijnberg, L. An Investigation of Water-Sensitive Oil Paints in Twentieth-Century Paintings. In *Modern Paints Uncovered: Proceedings from the Modern Paints Uncovered Symposium May 16–19, 2006 Tate Modern, London*; The Getty Conservation Institute, The National Gallery of Art, Thomas, L., Patricia, S., Jay, W.K., Michael, R.S., Eds.; Getty Publications: Los Angeles, CA, USA, 2006.
44. van den Berg, K.J.; Mills, L.; Burnstock, A.; Duarte, F.; de Groot, S.; Megens, L.; Bisschoff, M.; van Keulen, H. Water sensitivity of modern artists' oil paints. In Proceedings of the ICOM Committee for Conservation 15th Triennial Meeting, New Delhi, India, 22–26 September 2008. Allied Publishers.
45. van den Berg, K.J.; Burnstock, A.; Schilling, M. Notes on Metal Soap Extenders in Modern Oil Paints: History, Use, Degradation, and Analysis. In *Metal Soaps in Art, Conservation and Research*; Casadio, F., Keune, K., Noble, P., Van Loon, A., Hendriks, E., Centeno, S.A., Osmond, G., Eds.; Springer: Berlin/Heidelberg, Germany, 2019; pp. 329–342.
46. Tempest, H.; Burnstock, A.; Saltmarsh, P.; van den Berg, K.J. Sensitivity of oil paint surfaces to aqueous and other solvents. In *New Insights into the Cleaning of Paintings: Proceedings from the Cleaning 2010 International Conference Universidad Politécnica de Valencia and Museum Conservation Institute*; Marion, F.M., Elena, C.A., Robert, J.K., Eds.; Smithsonian Institution Scholarly Press: Washington, DC, USA, 2013; pp. 107–117.
47. Aviva, B.; van den Berg, K.J. Twentieth Century Oil Paint. The Interface Between Science and Conservation and the Challenges for Modern Oil Paint Research. In *Issues in Contemporary Oil Paint (ICOP)*; van den Berg, K.J., Kreuger, J., Heydenreich, G., Burnstock, A., Learner, T., Eds.; Springer: Amersfoort, The Netherlands, 2014; pp. 1–19.
48. Graczyk, A. *La Créole by Alexis Mérodack-Jeaneau, an Unexpected Witness for Painting Materials Circa 1910*; Book of Abstract; Futurahma: Pisa, Italy, 2016.